Available online at www.sciencedirect.com
ScienceDirect
Trans. Nonferrous Met. Soc. China 29(2019) 710−721
Transactions of Nonferrous Metals Society of China
www.tnmsc.cn

Microstructure, mechanical and tribological properties of A390/SiC composite produced by compocasting

Javad MOHAMADIGANGARAJ, Salman NOUROUZI, Hamed JAMSHIDI AVAL

Department of Materials Engineering, Babol Noshirvani University of Technology, Shariati Avenue, Babol 47148-71167, Iran

Received 17 June 2018; accepted 19 December 2018

Abstract: Aluminum A390 alloys reinforced with 10 wt.% SiC composite, were produced by the compocasting method. The effects of temperature, time, and stirring speed of this compocasting method on the microstructure, mechanical and tribological properties of composite were investigated. The results indicated that with increasing the rotational speed from 450 to 550 r/min, the distribution of the SiC particles becomes more uniform. A sudden increase in porosity due to gas absorption results in a downtrend of elongation with an increase in stirring speed from 550 to 650 r/min. Furthermore, as the stirring time increases, the amount of agglomerates of primary Si particles is reduced, and a more uniform microstructure of SiC and Si particles is formed. Although the fracture mode is a combination of both brittle and ductile fractures, the main mechanism of the fracture in the compocast sample is ductile. The formation of a protective layer at a high temperature can result in a very low wear rate as compared to a wear test performed at a low temperature. Optimal particle uniformity and mechanical properties were obtained at processing parameters of 610 °C, 550 r/min, and 20 min.

Key words: A390/SiC compocasting; composite; microstructure; SiC particles

1 Introduction

Aluminum matrix composites (AMCs), especially those with SiC particulate reinforcement due to unique properties like high wear resistance, low thermal expansion, and high specific strength, have recently gained attention in transportation industries [1−4]. These composites can be produced in a variety of ways; over the past decade, the application of the casting method has been more popular than other methods in these industries [5,6]. AMCs can be replaced unlike iron base parts, which can greatly reduce the weight of the components. Silicon carbide particles, as reinforcement particles in AMCs, have higher levels of hardness and lower price than most other ceramic reinforcements [7,8].

Al−Si hypereutectic alloys solidify in a wide range, making them suitable for composite fabrication using the compocasting method. Although agglomeration and clustering are inevitable in the compocasting process (as with other methods of casting), these can be minimized with precise control of the process parameters [9]. The main factor affecting the mechanical properties of these alloys (like A390) is the control over distribution, morphology, and particle size of primary and eutectic silicons [10].

There has been limited research on the construction of AMCs using hypereutectic aluminum alloys and ceramic reinforcement particles. GOO et al [11] investigated the effect of SiC reinforcement particle size on the mechanical properties of A390 alloy matrix composite produced by a mechanical stirrer in a semi-solid state. They found that the optimum temperature for mixing particles is exactly below the liquidus line and the resistance to wearing composites with larger particles is more than smaller ones. It was also reported that the presence of cavities in semi-solid composites, by creating a stress concentration at the location of the cavities, affects the strength of composites. WANG et al [12] investigated the effect of freezing of the silicon phase on SiC particles in aluminum hypereutectic composites. They found that in the freezing of these composites, primary silicon particles first nucleate onto SiC particles. It was reported that in the early stages of solidification, silicon particles are close to SiC particles; however, over time, SiC

Corresponding author: Salman NOUROUZI; Tel: +98-11-35501800; Fax: +98-11-35501802; Email: s-nourouzi@nit.ac.ir
DOI: 10.1016/S1003-6326(19)64981-2

particles are diverted and agglomeration of primary silicon particles may occur. EL MAHALLAWI et al [10] studied the construction of metallic field composites using the A390 alloy and TiO_2/Al_2O_3 particles by the rheocasting process. The results showed that the presence of reinforcing particles increases the hardness of aluminum alloy and the formation of a fine-grained structure. PRABU et al [13] investigated the effects of the speed and time of stirring on the A384 alloy matrix composite with SiC-reinforcing particles. They showed that by increasing the speed and time of mixing, a better distribution of reinforcing particles is obtained. It was also reported that porosity increases at the stirring speed of more than 700 r/min and hardness distribution varies in low stirring rates due to the heterogeneous distribution of the reinforcing particles.

Till now, there has been limited research on the compocasting of hypereutectic aluminum alloys, especially the A390 alloy using SiC-reinforcing particles. Factors that influence the compocasting process include wettability of the reinforcing particles, proper mixing (temperature, time, and stirring speed), size of the reinforcing particles, volume fraction of the reinforcing particles, mold temperature, and rate of solidification. The determination of optimal compocasting parameters has a fundamental role in obtaining the desired mechanical and tribological properties. In this work, we investigated the effects of stirring temperature, speed and time on the A390/SiC composite microstructure made by the compocasting method. Also, the effect of process parameters was studied to obtain desired mechanical and tribological properties.

2 Experimental

The chemical composition of A390 aluminum alloy is listed in Table 1. Figure 1 shows the SEM image of the as-received SiC particles with a mean size of 45 μm. To improve the wettability of SiC in molten aluminum alloy and to prevent the floating of SiC particles in the molten aluminum, a SiO_2 layer was formed by putting the SiC particles in a furnace at 900 °C for 5 h. The compocasting method was used for fabrication of A390/10wt.% SiC composite. The electrical furnace was used for melting alloy at a temperature of up to 750 °C in the first stage. In the second stage, the temperature of molten aluminum was reduced to 610−630 °C. Simultaneously, the preheated (at 600 °C) oxidized SiC particles were injected in graphite crucible while the molten metal was stirred by a mechanical stirrer. The semi-solid composite was poured into a metal mold. A single-factor experimental design was used for conducting the experiments. This means that for finding the effect of the given parameters, it varies through the levels while the others are keeping constant. Detailed casting parameters are given in Table 2.

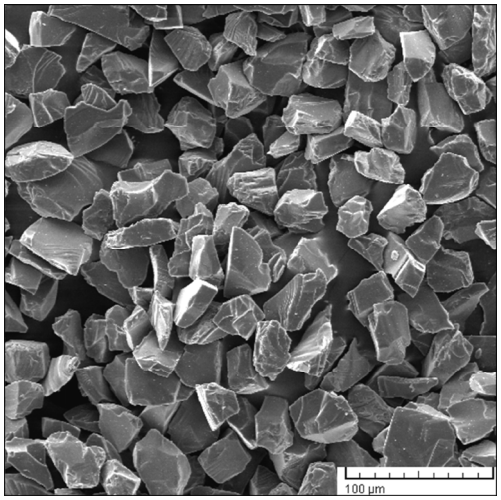

Fig. 1 SEM image of SiC powders used in this work

Table 1 Chemical composition of A390 aluminum alloy (wt.%)

Si	Cu	Mg	Fe	Mn	Zn	Ti	Cr	Ni	V	Pb	Al
18	4.2	0.31	0.64	0.29	0.06	0.02	0.02	0.01	0.01	0.01	Bal.

Table 2 Compocasting parameters used in experiments

Stirring speed/ ($r \cdot m^{-1}$)	Stirring temperature/°C	Stirring time/ min
450, 550, 650	610, 620, 630	10, 15, 20

Also, in order to compare the microstructure features, two samples (as-cast and semi-solid) without SiC particles were prepared. The as-cast sample was melted and poured at a temperature of about 750 °C; to prepare the semi-solid sample, it was poured in the mold after lowering the temperature from 750 to 620 °C and stirring for 15 min.

After solidification, metallographic samples were selected from the middle of the cast piece for the microstructure analysis. After cutting, the specimens were sanded with 180 grit sandpaper until 3000 and then polished for microstructure analysis. Porosity (η) of the resultant composite was calculated as follows:

$$\eta=(1-\rho/\rho_0)\times100\% \quad (1)$$

In the above equation, ρ and ρ_0 are densities of the composite and value obtained using the rule of mixtures, respectively. The density of the composite was calculated by Archimedes' principle [14]. An optical microscope and scanning electron microscopy (SEM) equipped with an energy-dispersive X-ray spectroscope (EDS) were employed for microstructure study of composites.

Vickers hardness of composites was measured on different points of each specimen with 98 N. To determine the tensile strength of composites, three flat tensile specimens for each condition were tested according to ASTM E8 using a SANTAM−600 Universal Testing Machine at room temperature and a constant crosshead speed of 0.5 mm/min. Dry sliding wear tests were performed to compare the wear properties of as-cast, stirred (semi-solid), and composite samples at ambient laboratory conditions. The wear tests were carried out using a pin on disc wear testing machine according to the ASTM G99−15 under a load of 10 N and at a distance of 1000 m. The pin was a rectangular cube with 5 mm × 5 mm × 6 mm (height). The square section of the pin was slid with a linear speed of 0.5 m/s on a counterface disc made of AISI/SAE 52100 steel with a hardness of HRC 60.

3 Results and discussion

3.1 Microstructure analysis of composites

Figure 2 shows the microstructures of A390/10wt.% SiC composites produced with various compocasting

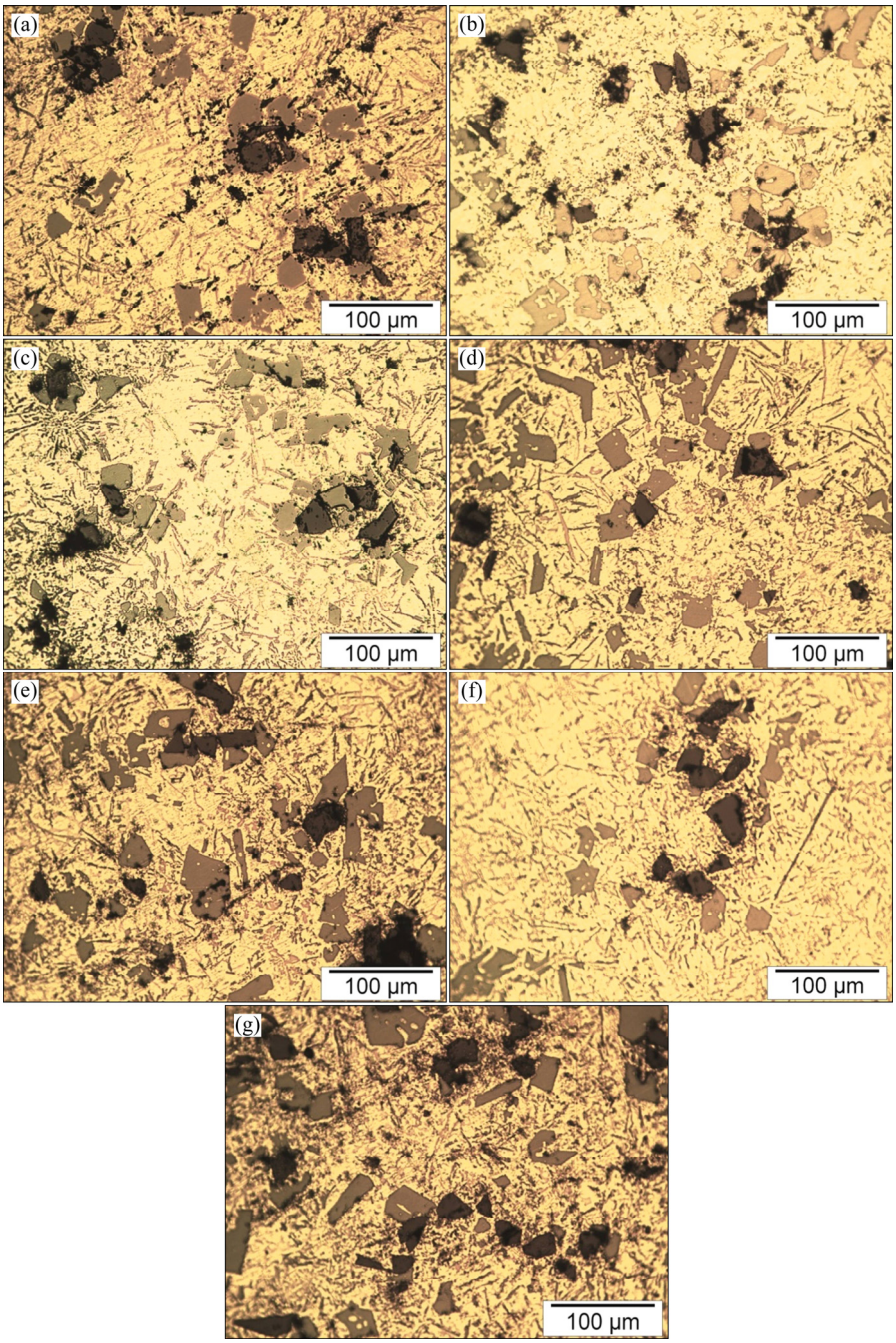

Fig. 2 Optical microscopy images of composite A390/SiC under different stirring conditions: (a) 550 r/min, 15 min, 630 °C; (b) 550 r/min, 15 min, 620 °C; (c) 550 r/min, 15 min, 610 °C; (d) 450 r/min, 15 min, 610 °C; (e) 650 r/min, 15 min, 610 °C; (f) 550 r/min, 10 min, 610 °C

process parameters including stirring speed, stirring time, and stirring temperature. Uniform distribution of particles in the matrix and minimizing porosity in composites play an important role in improving their mechanical properties. To achieve the best homogeneity of SiC particles in the matrix, the parameters of stirring must be studied. Particle uniformity was measured by the distribution factor (DF) by dividing the particle surface standard deviation on its mean particle surface fraction [15]. The particle surface standard deviation and the mean value were calculated by image analysis software. Non-uniform distribution of particles increases the distribution factor. As shown in Fig. 3(a), the DF value demonstrated that the uniformity of SiC particle distribution increased by decreasing the stirring temperature. By reducing the temperature, the distribution of particles is more uniform; this is due to the increase of solid fraction and subsequent increase of molten viscosity. Another issue is the oxidation of molten metal with increasing temperature, which leads to the formation of harmful compounds at the interface and agglomeration stages.

In Fig. 2, black and gray particles are SiC and primary Si, respectively. Considering the microstructure of composite samples, it can be seen that as temperature increases, both the agglomeration of SiC particles and the accumulation of primary Si particles around the SiC particles also increase (see Fig. 3(a)). It should be noted that although temperature increases, the amount of trapped gases reduces due to less composite viscosity; however, the agglomeration of SiC and primary Si particles in their surroundings leads to the formation of a cavity in the space between these particles. The morphology of the primary Si particles in all samples is polygonal, while the morphology of the Si-eutectic particles is flake-like, nucleating in the matrix of aluminum and around the primary Si particles. The important point is to reduce the amount of agglomerates of the primary Si particles in their surroundings by increasing the temperature. As the temperature of the composite increases, the primary Si particles move more easily to the SiC particles and accumulate around these particles due to the lower viscosity of aluminum matrix.

It was observed that by increasing the stirring speed from 450 to 650 r/min (Fig. 3(b)), SiC particle uniformity improved. This is due to the increase in shear stress by increasing the stirring speed. A stirring speed of 550 r/min can be considered as optimal in terms of the distribution of SiC and Si particles; this is considering the increase in agglomeration of primary Si particles around the SiC particles by increasing the stirring speed and subsequently reducing the uniform distribution of primary Si particles in the matrix of aluminum, as well as by increasing the porosity.

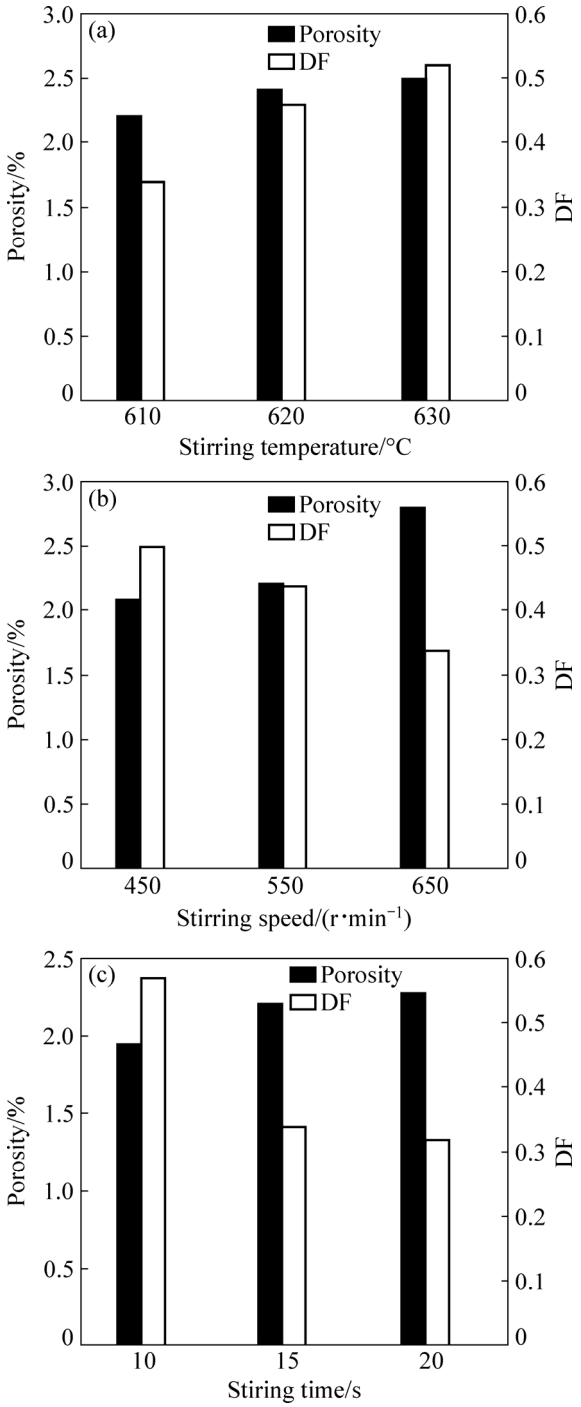

Fig. 3 Variation of porosity and DF with different stirring parameters: (a) Temperature; (b) Speed; (c) Time

By decreasing the stirring time, the amount of distribution of the SiC particles decreases (Fig. 3(c)). As the stirring time increases, the amount of agglomerates of the initial Si particles is reduced, and a more uniform microstructure of SiC and Si particles is formed. The important point is that porosity in the composite increases with stirring time; this is due to the increased gas absorption and oxidation of the melt. It is noteworthy that the effect of stirring speed, stirring time, and

temperature on the morphology and distribution of Si-eutectic particles in the microstructure is less than that of SiC and primary Si particles. According to the microstructure analysis, the major porosity available in the A390/SiC composites includes the porosity associated with SiC and primary Si particles, the porosity associated with SiC and primary Si particle clusters, and the microporosity in the aluminum matrix.

Figure 4 shows the back scattered electron image of the as-cast A390 alloy, A390 alloy stirred without SiC particles, and A390/SiC composite under stirring conditions of 550 r/min, 20 min, and 610 °C. As shown in Figs. 4, EDS analyses in all specimens determined α(Al), primary and eutectic silicon structures, and $CuAl_2$ and Al_5FeSi intermetallic compounds. There is no significant difference in the morphology of intermetallic compounds, eutectic structure, and primary Si particles in different specimens. However, it should be noted that the size of the primary Si particles in the as-cast structure is far greater than that in the other two specimens.

One of the important factors affecting the mechanical properties of the composite is the bond formed between reinforcing particles and matrix alloys. Figure 5 shows the interface between the SiC particle

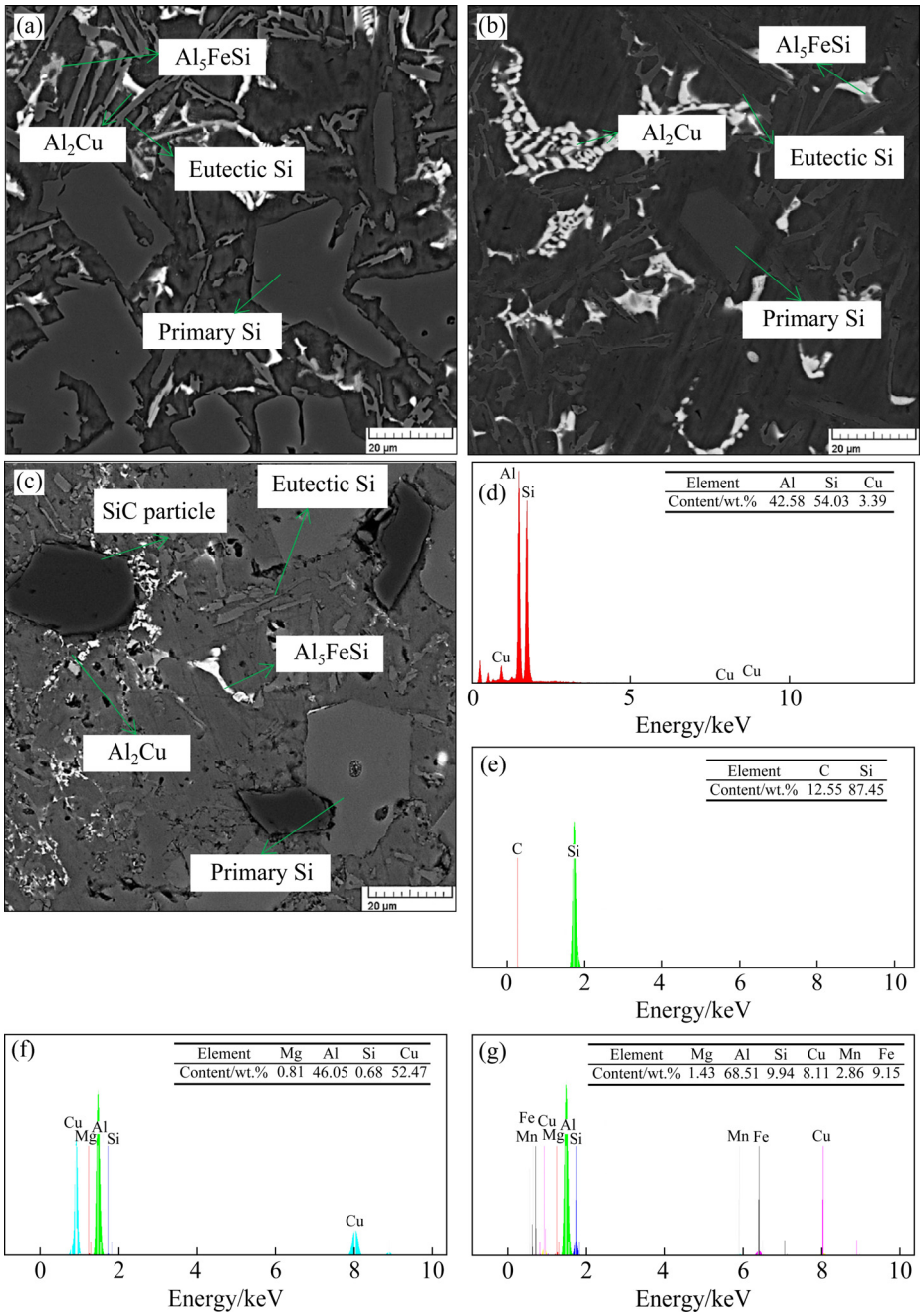

Fig. 4 Back scattered electron image of as-cast A390 alloy (a), A390 alloy stirred without SiC particles (b), A390/SiC composite under conditions of 550 r/min, 20 min, 610 °C (c), and EDS analyses of Si (d), SiC (e), Al_2Cu (f), and Al_5FeSi (g)

and the aluminum matrix in the A390/SiC composite with stirring parameters of 550 r/min, 20 min, and 610 °C. The interface is completely interconnected, indicating the wettability and good bonding of the SiC particles and the aluminum matrix. The EDS analysis performed at the interface (Fig. 5(b)) shows that the presence of oxygen is due to the oxidation of the surface of SiC particles before adding to the melt. The presence of magnesium and aluminum related to the aluminum matrix is also confirmed. The lack of identification of carbon by the EDS analysis is due to the low atomic number. It is also observed that copper, as an aluminum matrix element, is not seen around SiC particles. The absence of this element around the SiC particles is due to either the formation of Al_2Cu in the vicinity of SiC or its nucleation in a non-homogeneous manner on SiC particles.

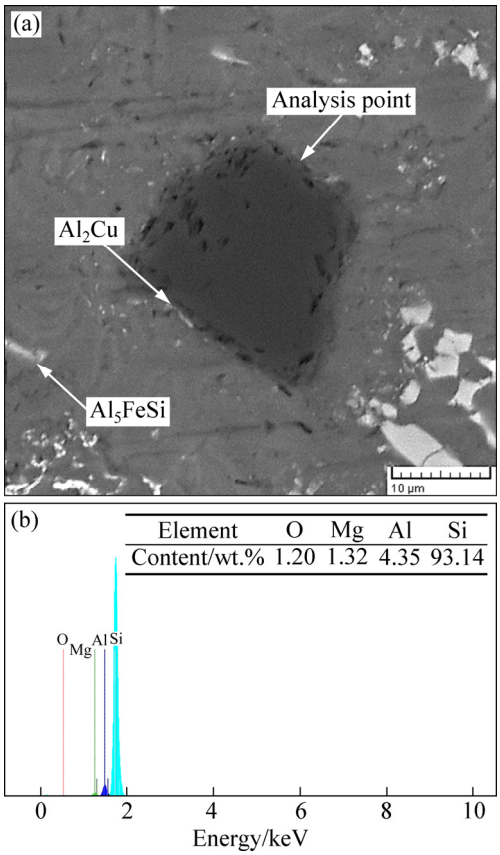

Fig. 5 SEM image (a) and EDS analysis (b) of interface between SiC particle and aluminum matrix in A390/SiC composite under conditions of 550 r/min, 20 min and 610 °C

3.2 Mechanical properties

The increasing hardness of the matrix by adding strong and stiffer particles is obvious, but the uniform distribution of particles and subsequently the uniformity of hardness are important. The average hardness of as-cast and stirred specimens without SiC particles is HV 87 and HV 92, respectively. Since process parameters play a fundamental role in the uniform distribution of particles in the matrix, it is necessary to obtain optimal parameters. The percentages of hardness distribution of specimens for different processing parameters are shown in Table 3. The results confirm the relationship between particle distribution and the average of composite hardness. By decreasing DF, the percentage of hardness distribution at intervals of less than HV 120 decreases, while in contrast, the percentage of hardness distribution at intervals of more than HV 120 increases. Therefore, the average hardness of composites increases with a decreasing distribution coefficient.

The ultimate tensile stress and elongation of the composites for various parameters of the compocasting process are shown in Fig. 6. Also, Fig. 7 shows the ultimate tensile stress, elongation, and tensile toughness of the composites versus the distribution factor of the SiC particles. The simultaneous optimal distribution of SiC particles and reduction of the porosity can increase strength, ductility, and toughness. Additionally, the particle cluster has a negative effect on tensile properties. When SiC particles accumulate locally in an area, porosity increases in that area, which is a place for crack initiation. Although, with increasing stirring time, the porosity in the structure increases a little, but the particle clustering becomes less. When particles are distributed more uniformly and less clustering happens, the elongation increases. By increasing the stirring time and decreasing the stirring temperature, the tensile properties of the A390/SiC composites were increased. Increasing the stirring temperature from 610 to 630 °C at a constant stirring time of 15 min and stirring speed of 550 r/min leads to a decrease of ultimate tensile stress (UTS) and elongation. It can be seen that UTS and elongation decreased by 11.4% and 15.2%, respectively. Increasing the stirring speed from 450 to 650 r/min increases the uniformity of SiC particle distribution, thereby increasing the strength and elongation. An important point is the downtrend of elongation with the increasing of stirring speed from 550 to 650 r/min. This observation can be related to a sudden increase in porosity at a speed of 650 r/min due to gas absorption. Also, as the stirring time increases, the strength and elongation of composite also increase.

One of the strengthening mechanisms in the composites is reinforced by SiC particles operated by load transfer from matrix to reinforcements [16,17]. The other type of strengthening is a result of microstructure changes of the composite [18]. The reinforcing particles act as obstacles to the motion of dislocations due to the incompatibility between the reinforcing particles and the

Table 3 Hardness distribution, standard deviation (S.D) and average of hardness at different processing parameters

No.	Processing parameter	Hardness distribution/%			S.D of hardness	Average of hardness (HV)
		>HV 110	HV 110−120	HV 120−130		
1	550 r/min, 15 min, 630 °C	45	35	20	8.66	111.92
2	550 r/min, 15 min, 620 °C	35	45	20	8.58	113.84
3	550 r/min, 15 min, 610 °C	25	50	25	8.32	116.68
4	450 r/min, 15 min, 610 °C	30	45	25	7.44	114.38
5	650 r/min, 15 min, 610 °C	30	35	35	9	115.31
6	550 r/min, 10 min, 610 °C	25	55	20	6.16	113.67
7	550 r/min, 20 min, 610 °C	10	20	70	6.27	121.76

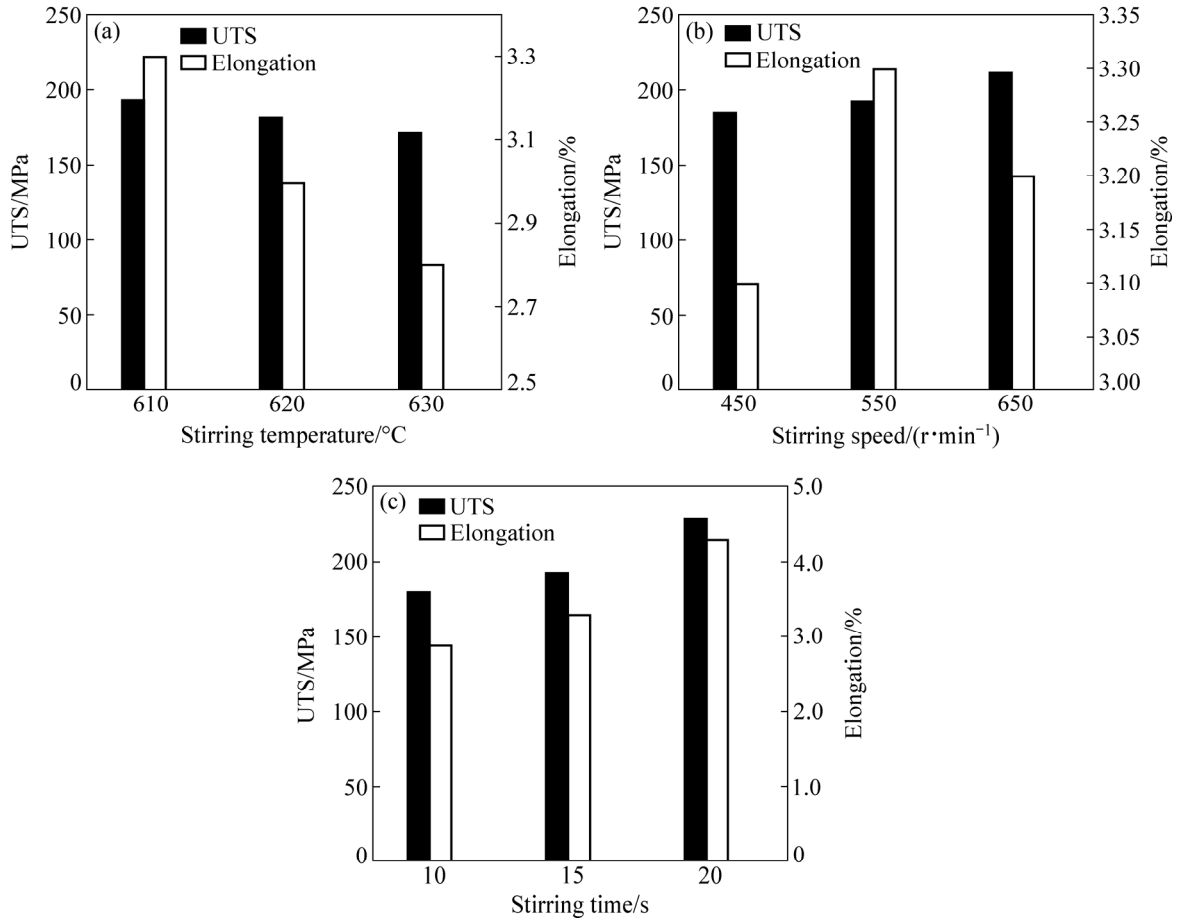

Fig. 6 Variation of ultimate tensile strength (UTS) and elongation with different stirring parameters: (a) Temperature; (b) Speed; (c) Time

metal matrix alloy. The presence of reinforcing particles causes geometric dislocations to occur in the interface area with the reinforcement particles. Another theory for increasing the strength of metal matrix composites is correlated to the increase in strength with the difference in the thermal expansion coefficient of the matrix and reinforcement particles that produce a high density of dislocation in the aluminum matrix (the thermal expansion coefficient of aluminum is about seven times the coefficient of SiC particles) [19]. This leads to the formation of residual stresses during the cooling of the composite from high temperatures at the time of the production process. The presence of these residual stresses leads to the aluminum matrix and reinforcement particles to be under tensile and compression stress, respectively. The creation of residual stresses increases the density of dislocations at the interface of matrix and reinforcement particles. By considering each of the aforementioned theories, the creation of a cellular structure of dislocations around SiC particles can be

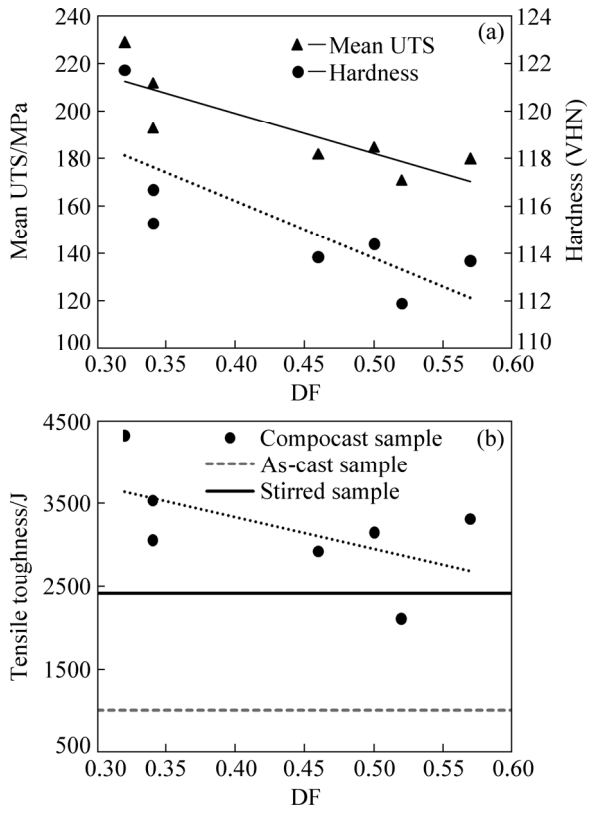

Fig. 7 Effect of distribution factor (DF) on mean ultimate tensile strength and hardness (a) and tensile toughness (b)

confirmed. Accordingly, by adding reinforcing particles, the amount of cellular structure around the reinforcement particles, the collapse of the cell structure, and the barriers to the movement of dislocations will increase. This action will increase the stress required for passing dislocation from the reinforcing particles and will slow down the movement of the dislocation, which will increase the strength and hardness of the composite.

Figure 8 shows the fracture surface of the as-cast, stirred, and compocast samples. According to Figs. 8(b), (d) and (f), both brittle features (red arrows) and dimples (white arrows) exist on the fracture surface. It can be concluded that the fracture mode is a combination of both brittle and ductile fractures. Also, more dimples in the stirred sample and especially in the compocast sample show that the main mechanism of a fracture is ductile. A comparison of as-cast, stirred, and composite samples shows that the size and sharp edge of primary Si particles are reduced, as well as the cracks in the SiC particles of the composite sample, which, as shown in Fig. 8(f) with the blue arrow, represent a strong bond between the SiC particles and the matrix. The presence of coarse particles of primary and eutectic Si, as well as their weak bond with the matrix (as shown with the dash arrow), will give rise to the formation of cracking and will be easier to expand.

3.3 Analysis of wear behavior

Figures 9(a−c) show the coefficient of friction (μ) of the following samples: as-cast A390 alloy, A390 alloy stirred without SiC particles, and A390/SiC composite with stirring parameters of 550 r/min, 20 min, and 610 °C at a distance of 1000 m. The coefficient of friction of the composite sample is less than that of the other two samples. There are many oscillations in the coefficient of friction of the as-cast sample. In the stirred sample without SiC particles, the coefficient of friction is slightly higher than that in the as-cast sample, but its oscillations are reduced due to the uniform distribution of silicon particles; however, the oscillation is high at a distance higher than 850 m, which indicates the change of wear mechanism. This is probably due to the detachment of silicon particles and the oxidation of aluminum because of rising temperatures at higher distances. In the as-cast sample, complete destruction takes place; this mechanism is a combination of adhesion wear and delamination, in which case severe plastic deformation occurs. As wear occurs in dry conditions, rising temperatures lead to softening of the base metal and delamination. High oscillation indicates adhesion wear.

Figures 10(a−c) show the SEM images of worn surfaces of stirred, compocast, and as-cast samples. In the as-cast sample, microcracks that are perpendicular to the sliding direction are nucleated near the surface at a certain depth, which is a result of shear effect. Due to the reciprocating load, the microcracks grow and propagate parallel to the wearing surface. As a result, macrocracks are formed and the as-cast bulk matrix peels off. Additionally, a large number of flake-like debris is placed between the pin and the disc, and a three-body abrasion occurs that results in an immediate increase in the friction coefficient. These microcracks do not exist in the composite sample (Fig. 10(c)). The grooves in the composite sample are shallower and wider. On one hand, resistance to plastic deformation in the composite sample increases due to the addition of SiC particles, which produce less microcracks. On the other hand, since SiC particles are distributed randomly in the aluminum matrix, if microcracks nucleate in the aluminum matrix, they will reach the SiC particles and stress concentration at the crack tip will be released [20]. Therefore, homogeneous particle distribution plays an important role in wear resistance. The important factor here is the bond between SiC particles and the matrix. The best condition for high wear resistance is that when SiC particles cannot be easily detached and there are few cuttings. Figures 9(d) and 10(d) show the coefficient friction and worn surface performance for sample A390/SiC composite tested at a temperature of 200 °C.

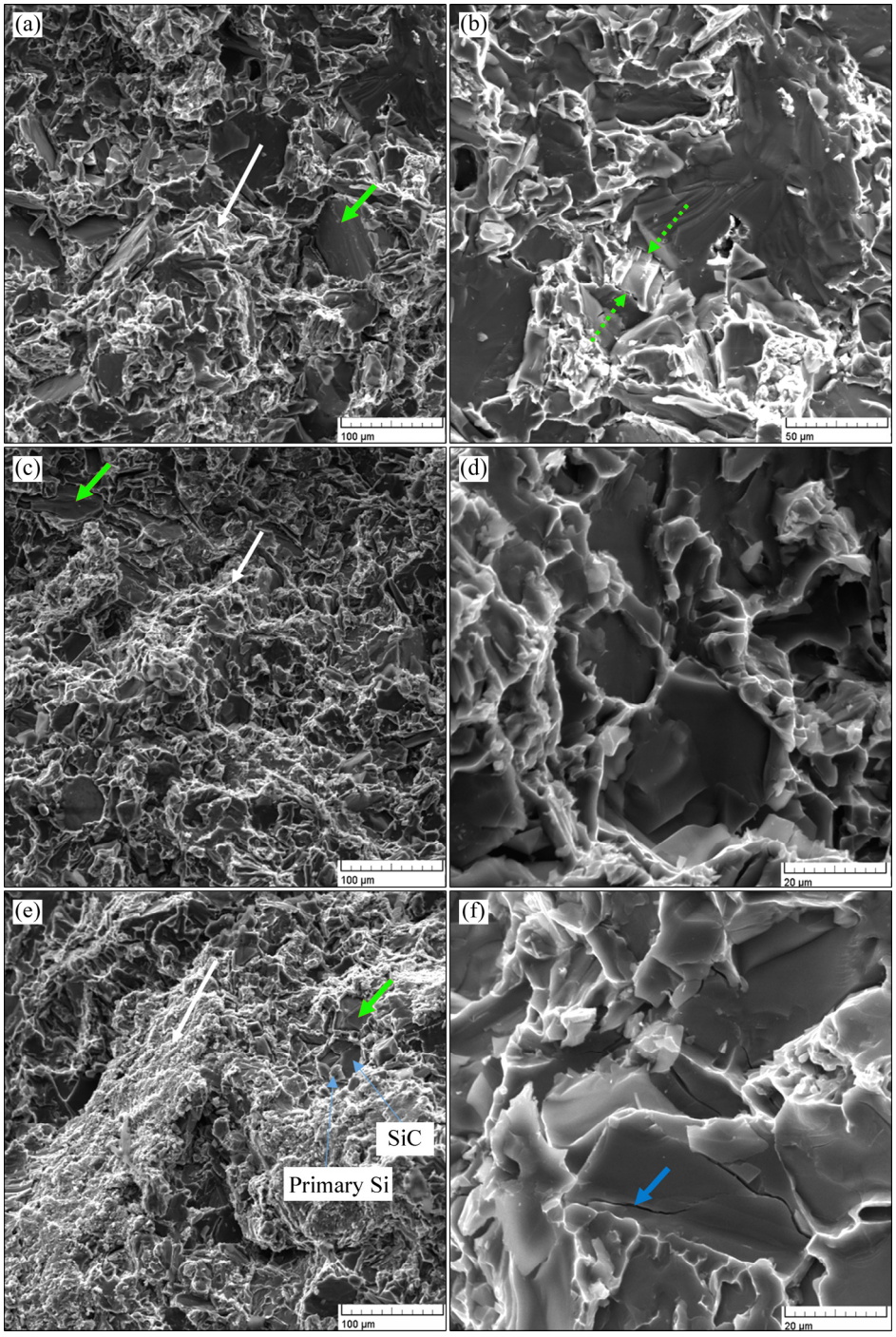

Fig. 8 SEM images showing fracture surface of as-cast (a, b), stirred (c, d), and compocast (e, f) samples

At a high temperature, the pin and abrasive disc surface have asperity-to-asperity contact. The first stage of wear is the detachment of composite materials by hard asperities present on the hard surface of the disc. When the wear continues, more softening of the pin material at high temperature occurs, resulting in the penetration of hard asperities on the surface of the disc; therefore, more materials will be detached from the pin. At a high temperature, softening of aluminum matrix results in weak bonding among the matrix, SiC and Si particles, and cracks will form leading to the pulling off of hard particles. These particles are trapped between the pin and the disk, and are crushed into finer particles. These fine particles and soft materials form a protective layer that reduces mass loss [21]. The results of the wear rate of the samples (Fig. 11) show that this protective layer can lead to a very low wear rate as compared to a wear test performed at a low temperature.

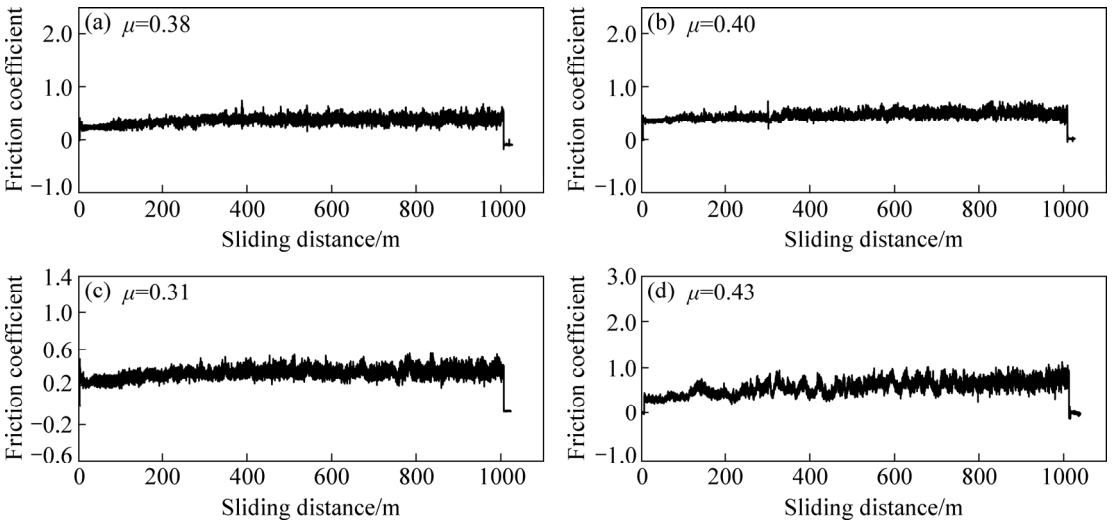

Fig. 9 Variation in coefficient of friction of as-cast A390 alloy (a), A390 alloy stirred without SiC particles (b), A390/SiC composite at 25 °C (c) and A390/SiC composite at 200 °C (d)

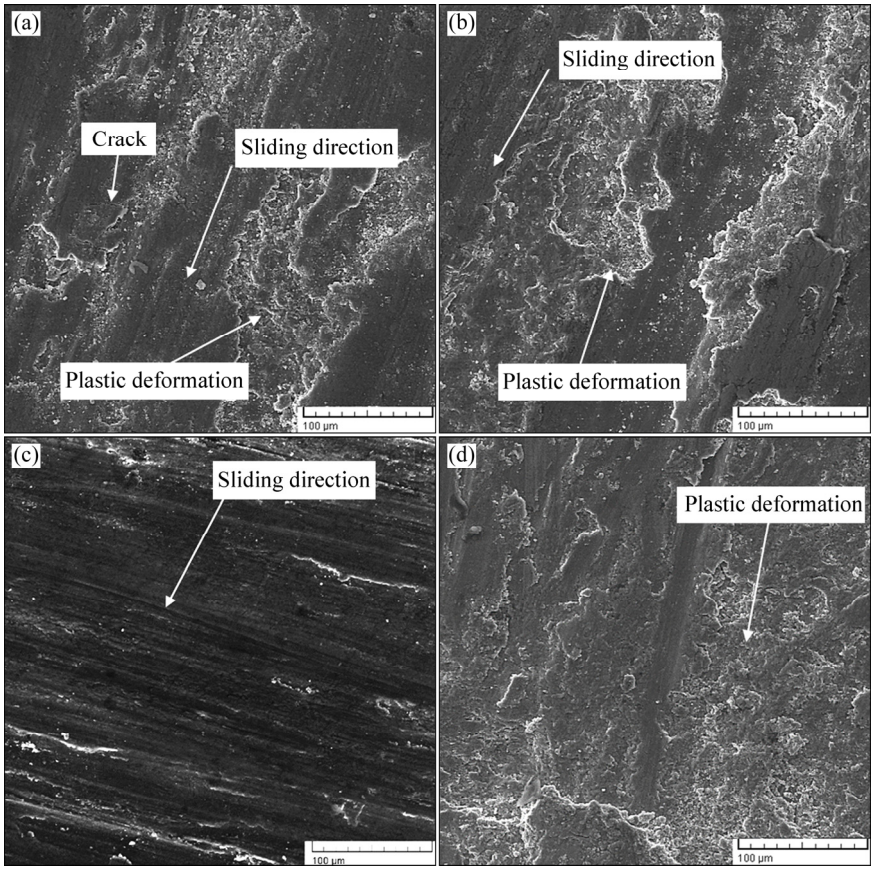

Fig. 10 SEM images showing worn surfaces of as-cast A390 alloy (a), A390 alloy stirred without SiC particles (b), A390/SiC composite at 25 °C (c) and A390/SiC composite at 200 °C (d)

4 Conclusions

(1) Decreasing the temperature and increasing the stirring time increase the uniformity of the particles. Optimal particle uniformity and mechanical properties were obtained under conditions of 610 °C, 550 r/min, and 20 min.

(2) The effect of stirring speed, stirring time, and temperature on the morphology and distribution of Si-eutectic particles in the microstructure is less than that in SiC and primary Si particles. According to

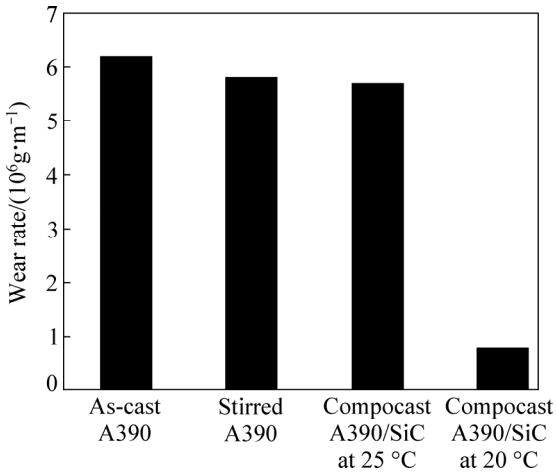

Fig. 11 Variation of wear rate of as-cast A390 alloy, A390 alloy stirred without SiC particles, A390/SiC composite at 25 °C, and A390/SiC composite at 200 °C

microstructure analysis, the major porosity available in A390/SiC composites includes porosity associated with SiC and primary Si particles, porosity associated with SiC and primary Si particle clusters, and microporosity in the aluminum matrix.

(3) By increasing stirring time and decreasing stirring temperature, the tensile properties of the A390/SiC composites increase. Increasing the stirring speed from 450 to 550 r/min increases the uniformity of SiC particle distribution, thereby increasing the strength and elongation. A sudden increase in porosity at a speed of 650 r/min due to gas absorption results in a downtrend of elongation with an increase in stirring speed from 550 to 650 r/min.

(4) The main mechanism of fracture in the stirred sample and especially in the compocast sample is ductile.

(5) Homogeneous SiC particle distribution plays an important role in wear resistance. The important factor here is the bond between SiC particles and the matrix. The wear grooves in the composite sample are shallower and wider. On the other hand, resistance to plastic deformation in the composite sample increases due to the addition of SiC particles which produce less microcracks.

References

[1] KHOSRAVI H, AKHLAGHI F. Comparison of microstructure and wear resistance of A356–SiC_p composites processed via compocasting and vibrating cooling slope [J]. Transactions of Nonferrous Metals Society of China, 2015, 25(8): 2490−2498.

[2] MAZAHERY A, SHABANI M O. Microstructural and abrasive wear properties of SiC reinforced aluminum-based composite produced by compocasting [J]. Transactions of Nonferrous Metals Society of China, 2013, 23(7): 1905−1914.

[3] AMOURI K, KAZEMI S, MOMENI A, KAZAZI M. Microstructure and mechanical properties of Al-nano/micro SiC composites produced by stir casting technique [J]. Materials Science and Engineering A, 2016, 674: 569−578.

[4] ALIZADEH M, PAYDAR M H, JAZI F S. Structural evaluation and mechanical properties of nanostructured Al/B4C composite fabricated by ARB process [J]. Composites Part B: Engineering, 2013, 44(1): 339−343.

[5] TZAMTZIS S, BAREKAR N S, BABU N H, PATEL J, DHINDAW B K, FAN Z. Processing of advanced Al/SiC particulate metal matrix composites under intensive shearing–A novel rheo-process [J]. Composites Part A: Applied Science and Manufacturing, 2009, 40(2): 144−151.

[6] AMIRKHANLOU S, NIROUMAND B. Synthesis and characterization of 356-SiC_p composites by stir casting and compocasting methods [J]. Transactions of Nonferrous Metals Society of China, 2010, 20(S): s788−s793.

[7] LADEN K, GUERIN J D, WATREMEZ M, BRICOUT J P. Frictional characteristics of Al–SiC composite brake discs [J]. Tribology Letters, 2000, 8(4): 237−247.

[8] HONG Soon-Jik, KIM Hong-Moule, HUH Dae, SURYANARAYANA C, CHUN Byong-sun. Effect of clustering on the mechanical properties of SiC particulate-reinforced aluminum alloy 2024 metal matrix composites [J]. Materials Science and Engineering A, 2003, 347(1): 198−204.

[9] KHOSRAVI H, BAKHSHI H, SALAHINEJAD E. Effects of compocasting process parameters on microstructural characteristics and tensile properties of A356−SiC_p composites [J]. Transactions of Nonferrous Metals Society of China, 2014, 24(8): 2482−2488.

[10] EL MAHALLAWI I, SHASH Y, RASHAD R M, ABDELAZIZ M H, MAYER J, SCHWEDT A. Hardness and wear behaviour of semi-solid cast A390 alloy reinforced with Al_2O_3 and TiO_2 nanoparticles [J]. Arabian Journal for Science and Engineering, 2014, 39(6): 5171−5184.

[11] GOO Byeong-Choon, KIM Myung-Ho. Characteristics of A356/SiC_p and A390/SiC_p composites [J]. Journal of Mechanical Science and Technology, 2012, 26(7): 2097−2100.

[12] WANG W, AJERSCH F, LÖFVANDER J P A. Si phase nucleation on SiC particulate reinforcement in hypereutectic Al−Si alloy matrix [J]. Materials Science and Engineering A, 1994, 187(1): 65−75.

[13] PRABU S B, KARUNAMOORTHY L, KATHIRESAN S, MOHAN B. Influence of stirring speed and stirring time on distribution of particles in cast metal matrix composite [J]. Journal of Materials Processing Technology, 2006, 171(2): 268−273.

[14] TAYLOR R P, MCCLAIN S T, BERRY J T. Uncertainty analysis of metal-casting porosity measurements using Archimedes' principle [J]. International Journal of Cast Metals Research, 1999, 11(4): 247−257.

[15] AKHLAGHI F, LAJEVARDI A, MAGHANAKI H M. Effects of casting temperature on the microstructure and wear resistance of compocast A356/SiCp composites: A comparison between SS and SL routes [J]. Journal of Materials Processing Technology, 2004, 155−156: 1874−1880.

[16] NARDONE V C, PREWO K M. On the strength of discontinuous silicon carbide reinforced aluminum composites [J]. Scripta Metallurgica, 1986, 20(1): 43−48.

[17] DAI L H, LING Z, BAI Y L. Size-dependent inelastic behavior of particle-reinforced metal−matrix composites [J]. Composites Science and Technology, 2001, 61(8): 1057−1063.

[18] MILLER W S, HUMPHREYS F J. Strengthening mechanisms in particulate metal matrix composites [J]. Scripta Metallurgica et Materialia, 1991, 25(1): 33−38.

[19] ARSENAULT R J, SHI N. Dislocation generation due to differences between the coefficients of thermal expansion [J]. Materials Science and Engineering, 1986, 81: 175−187.

[20] CAO Xiong, SHI Qing-yu, LIU Da-meng, FENG Zhi-li, LIU Qu,

CHEN Gao-qiang. Fabrication of in situ carbon fiber/aluminum composites via friction stir processing: Evaluation of microstructural, mechanical and tribological behaviors [J]. Composites Part B: Engineering, 2018, 139: 97−105.

[21] DAVID RAJA SELVAM J, DINAHARAN I, MASHININI P M. High temperature sliding wear behavior of AA6061/fly ash aluminum matrix composites prepared using compocasting process [J]. Tribology - Materials, Surfaces & Interfaces, 2017, 11(1): 39−46.

复合铸造 A390/SiC 复合材料的显微组织、力学和摩擦学性能

Javad MOHAMADIGANGARAJ, Salman NOUROUZI, Hamed JAMSHIDI AVAL

Department of Materials Engineering, Babol Noshirvani University of Technology, Shariati Avenue, Babol 47148-71167, Iran

摘　要：采用复合铸造法制备 10 wt.% SiC 增强的 A390 铝合金复合材料。研究复合铸造的温度、时间和搅拌速度对复合材料显微组织、力学性能和摩擦学性能的影响。结果表明，当转速从 450 提高到 550 r/min 时，碳化硅颗粒的分布更加均匀。由于气体的吸收，材料的孔隙率突然增大，导致随着搅拌速度从 550 增加到 650 r/min 时，伸长率下降。此外，随着搅拌时间的增加，原始硅颗粒团聚体的数量减少，显微组织中碳化硅和硅颗粒分布更加均匀。虽然复合铸造试样的断裂模式是脆性断裂和韧性断裂的复合，但其主要断裂机理是韧性断裂。与低温磨损试验相比，在高温下材料摩擦表面形成的保护层可导致极低的磨损率。得到最佳的颗粒均匀性和力学性能的工艺参数为：610 °C、550 r/min 和 20 min。

关键词：A390/SiC 复合铸造；复合材料；显微组织；SiC 颗粒

(Edited by Xiang-qun LI)